Catalysis Communications 184 (2023) 106795

Contents lists available at ScienceDirect

Catalysis Communications

journal homepage: www.elsevier.com/locate/catcom

Green hydroxyapatite-zeolite catalyst derived from steel waste as an effective catalyst for the hydrocarbon production via co-catalytic pyrolysis of sugarcane bagasse and high-density polyethylene

H. Hassan [a,*], B.H. Hameed [b]

[a] Waste Management and Resource Recovery (WeResCue) Group, Chemical Engineering Studies, College of Engineering, Universiti Teknologi MARA, Cawangan Pulau Pinang, 13500 Permatang Pauh, Pulau Pinang, Malaysia
[b] Department of Chemical Engineering, College of Engineering, Qatar University, P.O. Box: 2713, Doha, Qatar

ARTICLE INFO

Keywords:
Biomass
Plastic
Catalytic co-pyrolysis
Hydroxyapatite-zeolite
Bio-oil

ABSTRACT

Hydroxyapatite-zeolite (HAP-ZE) catalyst prepared from steel waste was utilised in *co*-catalytic pyrolysis of sugarcane bagasse (SB) and high-density polyethylene (HDPE) for bio-oil production. The highest bio-oil yield (71.19 wt%) was obtained at HAP-ZE to SB/HDPE ratio of 1:6, and mass ratio of SB to HDPE of 40:60. HAP-ZE favoured the production of hydrocarbon and alcohol and inhibited the production of acid. The acid sites promoted the hydrogenation and deoxygenation via hydrocarbon pool while the basic sites promoted the deoxygenation reactions via decarboxylation and decarbonylation. HAP-ZE large pores facilitates access of bulky pyrolyzates to active sites, promoting deoxygenation and hydrocarbons formation.

1. Introduction

The utilisation of an acidic catalyst is prevalent in catalytic co-pyrolysis (CCP) of biomass and plastic processes owing to its outstanding oxygen removal capabilities and superior cracking ability, primarily influence by its porosity and acidity [1]. However, its acidic properties can also lead to a significant generation of coke deposition due to the selective adsorption and subsequent rapid polymerization and condensation of sizable tar molecules on the outer surface of zeolites. As a result, the pore openings of zeolites become obstructed, leading to a significant decline in their catalytic activity and operational lifespan [2]. Base catalysts offer several benefits, including a reduced rate of active site poisoning, enhanced thermal stability, and proficient oxygen removal capability [3]. Multifunctional catalysts with acidic or basic properties either bifunctional or dual functional catalyst received much attention in complex co-pyrolysis process as it can catalyzed more than one type of reaction to produce targeted compounds [4,5]. Zhang et al. [6] stated that bifunctional catalysts that possess acid and base properties have shown the best balance between the quality and quantity of pyrolysis oil. Yang et al. [2] stated that the integration of acid and base catalysts can enhance the dehydration reaction, as well as the formation of low molecular weight products, thanks to the existence of neighbouring acid and base sites. The presence of base catalysts facilitates the breakdown of oxygenates, allowing them to effortlessly permeate into the cavities of acid catalyst. Subsequently, the oxygen-containing compounds undergo a breakdown and oxygen elimination reaction by means of the acid catalyst, leading to their conversion into aromatic hydrocarbons.

Research works in the recent decade have focused on the utilisation of low-cost materials, such as red mud [7], rice husk ash, spend FCC catalyst and natural zeolite [8], and spent bleaching clay [9] as catalysts for the deoxygenation of pyrolysis oil. The utilisation of these materials as green and environmentally catalyst could reduce the total production cost and encourage the use of sustainable resources. Electric arc furnace slag (EAFS) is a type of slag produced when recycled scrap is melted in an electric arc furnace. Most of this waste will end up in landfills, which can be hazardous to both humans and the environment due to its dusty nature, and the accumulation of heavy metals in groundwater and soil, including CO_2 emission [10]. EAFS typically contains high CaO content between 25 and 47 wt% [11], which could be the precursor for hydroxyapatite catalyst. Hydroxyapatite [$Ca_{10}(PO_4)_6(OH)_2$] can be characterised by alkaline in nature. It is widely used in catalysis due to its special features, which include being thermally stable, excellent acid-base properties, and good surface properties due to its ability to undergo cation and anion exchanges [12]. However, the application of this material in pyrolysis remains limited due to the low deoxygenation

* Corresponding author.
E-mail address: hamizura179@uitm.edu.my (H. Hassan).

https://doi.org/10.1016/j.catcom.2023.106795
Received 22 August 2023; Received in revised form 20 October 2023; Accepted 2 November 2023
Available online 4 November 2023

activity and aromatisation resulting from its low surface area and acidity. To address these limitations, hydroxyapatite-zeolite composite (HAP-ZE) derived from EAFS was synthesised in this study by using the CaO, SiO_2, and Al_2O_3 sources of EAFS. This composite could act as a bifunctional catalyst that possesses acid and base active sites. The introduction of zeolite into the hydroxyapatite matric could increase its acidity and enhance its catalytic activity.

Biomass has been recognised as the fourth largest energy system in the world, which can be converted into various form of renewable energy, including bio-oil, biochar, and syngas [13]. It is anticipated that by 2050, approximately 15% to 50% of the global primary energy demands could be supplied by lignocellulosic biomass [14]. In addition, biomass plays a crucial role in mitigating carbon emissions because of its carbon neutral [15]. Sugarcane bagasse (SB) ranks as one of the most prevalent agricultural byproducts with the annual consumption of 540 million tons worldwide. Typically, about 280 kg of SB has been produced for each ton of sugarcane processed [16]. SB contains cellulose (45%–55%), hemicellulose (20%–25%), lignin (18%–24%), ash (1.3%), and other components (2.8%) which can serve as a plentiful and environmentally sustainable biomass resource for the generation of energy and chemical compounds [17].

Pyrolysis is a thermal conversion technology that is recognised as one of the most economical, reliable, and effective methods to produce high-yield value-added fuels from biomass waste [18]. However, the high oxygen content and hydrogen deficiency of biomass may engender low quality bio-oil with high oxygenates (35–60 wt%), such as acids, alcohols, ester, aldehydes, ketones, and phenols, high water content (15–30 wt%) and viscosity, corrosiveness, poor stability, low pH (2 to 2.5), and low calorific value (16.6–19 MJ/kg) [19]. Ghai et al. [20] stated that feedstocks with hydrogen to carbon ratio (H/C_{eff}) of <1 are arduous and non-viable to be transformed into high-value products over acidic catalysts due to rapid poisoning and deactivation.

Recent studies have shown that addition of hydrogen-rich polymer such as plastic into biomass pyrolysis offers a promising approach to improve the quality and quantity of bio-oil resulting from the positive synergistic effect, and the outstanding deoxygenation and cracking performance [21]. Plastic could serve as a hydrocarbon pool that releases large amounts of H^+ and H_2, which can stabilise the reactive radical intermediates for the enhancement of aromatic selectivity, and the prevention of char and coke. Among plastic waste, high-density polyethylene (HDPE) is extensively employed as a supplementary substance for co-pyrolysis owing to its notable attributes such as a high hydrogen-carbon ratio (H/C) and minimal presence of nitrogen and oxygen [13].

In the present work, the catalytic potential of low-cost HAP-ZE composite that possesses acid-base properties was investigated in the CCP of SB and HDPE waste mixture. The efficiency of this catalyst was evaluated on the product yield and condensable compounds of bio-oil. As far as we know, HAP-ZE bifunctional catalyst has yet to be documented in the CCP of plastic and biomass waste. Thus, the properties of HAP-ZE and its influences on the product yield and quality of bio-oil were analysed in this study. The influences of catalyst-to-raw-material ratio (1:10, 1:8, 1:6, 1:4, and 1:2), and SB to HDPE ratio (100:0, 80:20, 60:40, 40:60, and 0:100) on the product yield and condensable compounds were investigated.

2. Experimental

2.1. HAP-ZE synthesis

Electric arc furnace slag (EAFS) was collected from a local industry in Pulau Pinang. Prior to synthesis, the EAFS was crushed using a cone and jaw crusher, followed by ball milling at 50 rpm, and sieved through 100–125 μm mesh to be used in catalyst synthesis. Then, 10 g of raw EAFS was dissolved in a predetermined volume of 1.0 M H_3PO_4 (85% purity, Sigma Aldrich) aqueous solution under continuous stirring. Preventing prolonged agitation was essential to impede the development of gel-like hydrous calcium phosphate when using lower solid/liquid ratios. A fixed volume of 1 M H_3PO_4 was used to keep the Ca/P molar ratio constant at 1.6667, which is the composition of the hydroxyapatite. Then, a specific volume of $Na_2Si_3O_7$ (Sigma Aldrich) that acted as a silica source was added into the mixture to balance the Si/Al ratio to 30. Next, 30 mL of 2 M NaOH (99% purity, Sigma Aldrich) aqueous solution was slowly poured into the mixture, which was constantly stirred at 60 °C for 3 h. NaOH was utilised as it can activate carbon and aid the synthesis of zeolites via hydrothermal treatment. [22]. The mixture was transported to a stainless-steel Teflon-lined autoclave, then subjected to heating at 100 °C for 48 h. Following the hydrothermal reaction, the resultant product was filtered and rinsed using deionised water until neutral pH. Then, it was dehydrated in the oven at 105 °C and heat-treated at 500 °C for 5 h to eliminate organic precursors and water. The prepared catalyst was denoted as hydroxyapatite-zeolite (HAP-ZE).

2.2. HAP-ZE characterisation

The N_2 physisorption was conducted using the Quantachrome, Autosorb surface area and pore size analyzer. The average pore width and pore size distribution of catalyst were calculated by BJH method whereas the pore volume and surface area were determined by BET method. X-ray diffraction (XRD) analysis of HAP-ZE was conducted using a Philip PW170 diffractometer that was operated at 40 kW and Cu-Kα radiation. The diffraction patterns were analysed within 2θ scan range of $10^\circ \leq 2\theta \leq 90^\circ$. The diffractograms offered more information on the crystallinity of the sample and illustrated intensity as a function of the diffraction angles. The Xpert Highscore Plus software was utilised for phase identification. The temperature-programmed desorption of ammonia (NH_3-TPD) was conducted using a Micromeritics AutoChem II Chemisorption Analyzer, armed with a thermal conductivity detector (TCD). The scanning electron microscope (SEM) was conducted using a Quanta FEG 450, armed with Energy Dispersive X-ray (EDX) (Oxford Instrument X-Max) to investigate the elemental and surface morphology of catalyst.

2.3. Pyrolysis procedure

The experiments were carried out in a fixed-bed reactor constructed of stainless steel. The internal diameter and height of the reactor are 5 mm and 700 mm, respectively. A two-stage pyrolysis arrangement was utilised, whereby the SB-HDPE mixture and the synthesised catalyst were separated by quartz wool to avoid immediate contact among them. The vapours coming from SB-HDPE mixture were passed through the catalyst to undergo further cracking and deoxygenation reaction. In a batch experiment, a specific quantity of catalyst and 6 g of SB-HDPE mixture in a mass ratio of 60:40 were loaded into the main pyrolysis unit. The reactor temperature was gradually increased at a rate of 10 °C/min until reaching the desired temperatures of 600, °C. To ensure complete pyrolysis of the feedstock, the operating temperature was sustained for a duration of 45 min. A carrier gas of high-purity nitrogen (99.99%) was employed, flowing at a rate of 250 mL/min. The liquid product, which comprised of aqueous and organic phases, was collected in two consecutive collectors, namely, the wax collector and the condenser. To maintain a temperature of 170 °C, the wax collector was equipped with a wax collector heater, while the condenser, immersed in an ice-cube bath, was maintained at −5 °C. Since a two-stage pyrolysis arrangement was used in this study, the SC-HDPE mixture was separated from the catalyst using quartz wool. The char by-product was collected from the feedstock layer, and this residue was measured using a weighing balance. The liquid yield was measured by assessing the change in mass of the liquid in the collector prior to and following pyrolysis. The yield of gas was estimated by mass balance method. The bio-oil, char, and gas yield were determined using Eqs. (1) to (3):

$$\text{Liquid yield (wt.\%)} = \frac{\text{Mass of liquid product}}{\text{Weight of total feedstock}} \text{ x } 100\% \quad (1)$$

$$\text{Char yield (wt.\%)} = \frac{\text{Mass of } char}{\text{Weight of total feedstock}} \text{ x } 100\% \quad (2)$$

$$\text{Gas yield (wt.\%)} = 100 - (\text{liquid yield} + char \text{ yield}) \quad (3)$$

2.4. Chemical analysis of bio-oil

GC/MS (Perkin Elmer Clarus 600/600 T) was employed to analyse the reactor outlet compound mixture. The system was set to start at 50 °C, hold for 2 min, then ramp to 280 °C at a heating rate of 5 °C/min and maintained for 20 min. The interface temperatures and injector were programmed at 300 and 250 °C, respectively. For the mass spectrometer measurements, the voltage and detection range (m/z) of mass spectrometry was set at 70ev and 50–400 amu, respectively. The size of the injected sample was 1 μL, with a split ratio of 2:1. High purity helium was utilised as the transport gas, flowing at a rate of 1.0 mL per minute. The compounds present were identified by comparing the spectral data to the NIST compound library. A semi-quantitative method was utilised to acquire the relative content of individual compound in pyrolysis vapours, by quantifying the chromatographic area percentage. The calorific value of the bio-oil was determined using a Bomb Calorimeter (IKA C200) following the ASTM D240–02 method.

3. Results and discussion

3.1. Characterisation of synthesised HAP-ZE catalyst

Fig. 1 shows the X-ray diffraction (XRD) profile of the synthesised HAP-ZE. The successful synthesis of HAP-ZE composite from the slag was confirmed by the good match of the peaks that belonged to the Faujasite-type (FAU) zeolite phase and the hydroxyapatite (HAP) phase. The peaks found at 25.96°, 31.90°, 39.44°, 46.75°, and 49.69° indicated the structure of crystalline hydroxyapatite ($Ca_5(PO_4)_3(OH)$), as reported in the JCPDS reference pattern (No. 090432) [23]. In addition, the three peaks located at 23.86°, 29.05°, and 35.38° can be assigned to the Faujasite-Ca zeolite, which implied the incorporation of zeolite into hydroxyapatite [24].

The results of the morphological and elemental analyses of HAP-ZE are shown in Fig. A1(a). The SEM image of HAP-ZE shows a mixture of two morphologically distinct crystals on the micro-scale. The spherical crystals, which were evenly dispersed on the rough surface, were identified as FAU-type zeolites [25]. Meanwhile, HAP is attributed to the larger, irregular flake-shaped particles with rough external surface (Fig. A1(b)), which are partially distributed onto the zeolite crystals. Non-simultaneous crystallisation was believed to have produced such morphology, with the formation of HAP occurring first, followed by the growth of zeolite crystals on the rough HAP surface [24]. The EDX results (inset Fig. A1(a)) show that the synthesised HAP-ZE contains Si, Al, Ca, P, Na, and O as the key components. The presence of Si and Al in the HAP-ZE composite confirmed the presence of zeolite, while the existence of Ca, P, and Na components verified the existence of HAP. Hence, the synthesised HAP-ZE catalyst could be considered as zeolite and hydroxyapatite composites. The EDX result showed that the HAP-ZE have a Ca/P ratio slightly higher than 1.67, suggesting that they are predominantly basic [26].

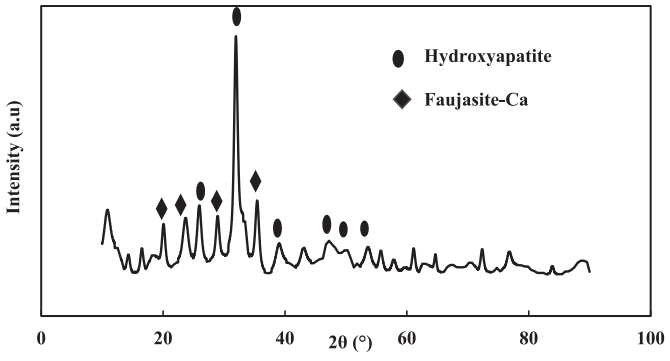

Fig. 1. XRD profile of HAP-ZE.

Physical characteristics, namely, specific surface area, pore diameter, and pore volume of HAP-ZE are summarised in Table A1. The pore volume and BET surface area of HAP-ZE, as analysed in this study, were 0.18 cm^3/g and 103.93 m^2/g, respectively. The BET surface area achieved by HAP-ZE was higher than the BET surface area of hydroxyapatite-zeolite derived from blast furnace slag [27]. The pore size of HAP-ZE, as quantified by BJH, was 9.15 nm, indicating a mesoporous material. The meso-porosity of the HAP-ZE and the larger pore opening would have increased the diffusion of a broader range of feedstock intermediates (produced at the early phases of pyrolysis) into the catalyst pore channel. The acidic sites on the catalyst would then aid the formation of higher value compounds. The catalyst's superior catalytic activity and prolonged lifespan were mainly attributed to the external acid sites on the mesopore walls, which outperformed the internal acid sites by exhibiting slower deactivation [28].

The pore size distribution and N_2 adsorption-desorption isotherm of the HAP-ZE catalyst are presented in Fig. 2. The HAP-ZE exhibited a type IV isotherm and H2 hysteresis loop, which occurred in the range of $0.4 < P/Po < 0.97$, signalling capillary condensation in the inter-crystalline mesopore void spaces [29]. Irregular distribution of pore structure, shape, and size of the materials signified the H2 hysteresis loop, as associated with highly mesoporous characteristics [30]. The BJH pore distribution of the HAP-ZE (inset Fig. 2) reveals a sharp peak in the mesopore region, with an average pore diameter of 6.52 nm.

The concentration, strength, and types of acid sites of HAP-ZE catalyst was analysed using NH_3-TPD technique. The low temperature peak on NH_3-TPD profile represented the weaker Brönsted acid sites and the non-framework Lewis acid sites, while the high temperature peak corresponded to stronger Brönsted acid sites [31]. The NH_3-TPD spectra of HAP-ZE is shown in Fig. 3. The HAP-ZE showed an intense ammonia desorption peak at 128 and 604 °C, which were ascribed to the desorption of ammonia molecules at strong and weak acid sites, respectively. These results indicated that HAP-ZE has both Brønsted and Lewis acid sites. Based on the quantification of the desorbed ammonia molecules, the overall amount of acid sites on HAP- ZE was found to be 0.18 mmol/g, and the quantified area under the two peaks indicated a distribution of 55% of weak acidity and 44% of strong acidity.

3.2. Influence of HAP-ZE to SB/HDPE ratio on pyrolytic products

The product yield and condensable compounds under different catalyst-to-feedstock ratio (HAP-ZE-to-SB/HDPE ratio) is illustrated in Fig. 4(a) and (b). The amount of catalyst was varied from 1:10 to 1:2. The SB-to-HDPE ratio and temperature were set at 60:40 and 600 °C, respectively. The results showed that the yield of bio-oil was first amplified when the HAP-ZE to SB/HDPE ratio was raised from 1:10 to 1:4. Then, the yield declined with additional increase of catalyst content to raw material ratio. The pyrolysis of bio-oil achieved the highest yield of 71.19 wt% with catalyst to raw material ratio of 1:4. This result is consistent with the finding claimed by Tan et al. [3], which found that the bifunctional catalyst derived from electric arc furnace slag (AS-EAF) and oil palm ash (AS-OPA) that are rich in Fe, Ca, Si, and Al could accelerate the production of bio-oil due to their excellent cracking activity. AS-EAF generated a higher gas yield as it contains higher amount of metal, such as calcium and iron, which are efficient in dehydrogenation and cracking of tar into smaller molecules.

The obtained bio-oil yield in this study was higher than our previous study (63.69 wt%) during the co-pyrolysis of SB and HDPE [32]. In

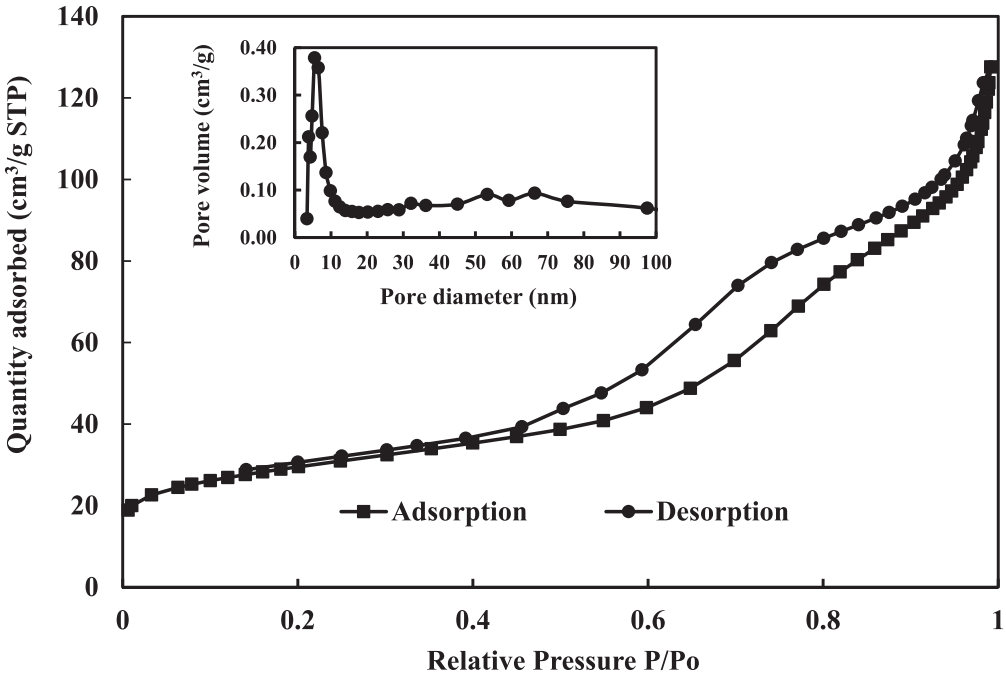

Fig. 2. Nitrogen adsorption desorption isotherms and pore size distribution of HAP-ZE.

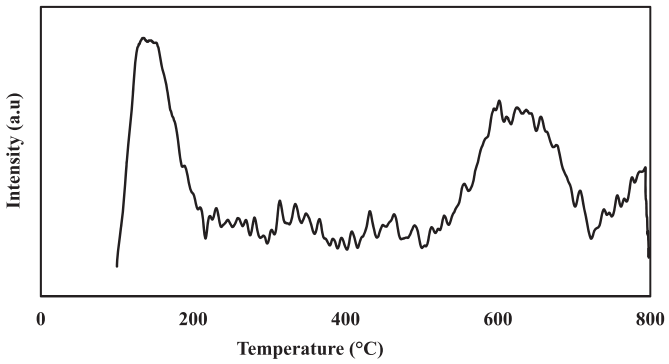

Fig. 3. NH_3-TPD plot of HAP-ZE.

catalytic co-pyrolysis over bifunctional catalyst such as HAP-ZE, the large molecular compounds were cracked into smaller compounds when the pyrolytic gas are in contact with base sites (HAP-ZE) which enhanced the accessibility of these molecules to the acid sites of the catalyst (zeolite). At the acid sites, the smaller molecules undergo further cracking and deoxygenation, which result in the decomposition of oxygen-containing compounds and reduction of undesired byproduct production. This leads to an increase in the yield of bio-oil. Zhang et al. [6] claimed that the bifunctional catalyst demonstrated the best balance between deoxygenation and liquid yield.

On the contrary, with an increase in the HAP-ZE to SB/HDPE ratio, the gas yield exhibited an increase, whereas the char yield experienced a decrease. The augmentation of the catalytic thermal cracking led to the enhanced transformation of pyrolysis vapours to gas, which was responsible for the increased gas yield and subsequently, reduced liquid yield. Zhao et al. [33] stated that the residence time of the pyrolysis vapour that passed through the catalyst pore was extended when the catalyst loading was increased, which lowered the production of bio-oil while increasing the yield of gas.

On the other hand, the decreased char yield was caused by the promoted hydrogen transfer reaction from HDPE to SB induced by HAP-ZE, which could suppressed the creation of coke on the surface of the catalyst as reported by Wang et al. [34] in the CCP of HDPE and waste vegetable oil over zirconium dioxide-based polycrystalline ceramic foam catalyst. Rocha et al. [35] reported that a slight decrease in char yield of the CCP of biomass containing plastic may possibly be ascribed to the effect of macromolecule fragmentation on the outer surface of the catalyst that generated smaller molecules. The smaller fragments could have then pass through the pore structure of the catalyst to undergo certain reactions, which consequently improved the yield of liquid and lowered the yield of char.

The presence of catalysts helps to augment the production of upgraded fuels, or chemicals by enhancing the cracking and deoxygenation reaction of the co-pyrolysis vapour that passes through its layer. Based on Fig. 4 (b), the alcohol proportion was increased by increasing the HAP-ZE-to-SB/HDPE ratio. When the catalyst to raw material proportion was enhanced, the overall amount of acid sites was substantially increased, which favoured the degradation of hemicellulose and cellulose to form alcohol. The primary identified components of alcohol were linear long-chain alcohols, namely, 1-Decanol, 2-hexyl-,1-Eicosanol, and 1-Heptacosanol. These long-chain alcohols resulted from the interaction between H radicals, which stemmed from HDPE polymerization, and SB-derived hydroxyl radicals. Moreover, the high surface area of HAP-ZE (Table S1) could have led to a bigger number of available Lewis acid sites, which could help accelerate the formation of linear long-chain alcohol. Catalysts with high surface areas and high thermal stability, with remarkable accessibility to available catalytic sites, could promote the desired reaction with high product yield and selectivity [36].

The addition of HAP-ZE had promoted the production of hydrocarbons, mainly olefins, and reduced the SB-derived oxygenated compounds. The hydrocarbons yield increased from 38.14% to 43.18% as the HAP-ZE to SB/HDPE ratio increased from 1:10 to 1:6 due to the increased number of active sites for acid or base-catalyzed deoxygenation reactions to transform oxygenated compounds to hydrocarbons. The results are in good agreement with the previous finding reported by Ryu et al. [37]. The authors also reported that catalysts with a larger BET surface area and pore volume, together with a better balance of acid and base, can have a positive influence on the production of valuable chemicals, including aromatics, furans, and phenols.

The addition of HAP-ZE had enhanced the catalytic decomposition of

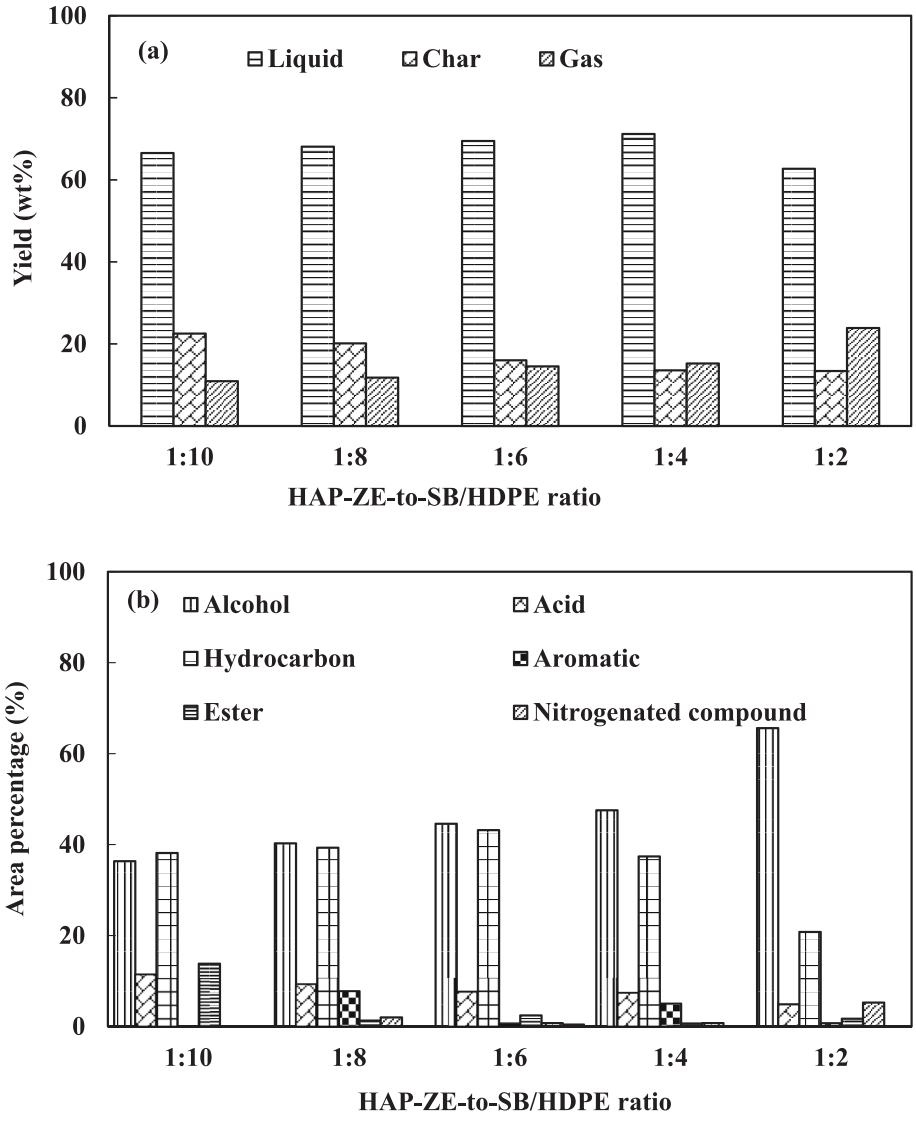

Fig. 4. Influence of HAP-ZE-to-SB/HDPE ratio on (a) product yield and (b) condensable compounds of CCP of SB and HDPE over HAP-ZE.

SB and HDPE intermediates, and the deoxygenation reaction of SB-derived oxygenates with HDPE-derived free radical via hydrogenation and dehydration reactions over its active sites. The catalytic decomposition of SB was able to produce different types of oxygenates, including acid, ketone, aldehyde, and alcohol. Meanwhile, the direct decomposition of HDPE via β-scission and carbonium ion had produced large amounts of olefins. These oxygenates, or "hydrocarbon precursor", along with HDPE-derived intermediates of olefin, had diffused into the porous HAP-ZE and underwent deoxygenation reactions, which included dehydration, decarbonylation, and decarboxylation, thus, resulting in a carbocation hydrocarbon pool. The HDPE-derived olefins acted as hydrogen contributors and amplified the concentration of hydrogen within the hydrocarbon pool, which further transformed the oxygen-containing compounds into hydrocarbon. The research study by Sekyere et al. [5] also found that the yield of hydrocarbons increased when acid-base catalyst were used in catalytic *co*-pyrolysis of pine and low-density polyethylene (LDPE). The introduction of base catalyst (CaAl) aid in the decomposition of large-oxygenated compounds that leads to a positive synergistic effect in the deoxygenation of produced bio-oil. The cracked molecules can easily access the active sites of acid catalyst (zeolite) and undergo further cracking to form light olefins and aromatics. The authors also reported that the arrangement of catalysts plays a vital role in the production of benzene, toluene, xylene (BTX), and light olefins. Acid-base tandem catalysis mode had the highest hydrocarbon yield as the pyrolytic gas contacted acid sites (zeolite) first, followed by the base site (CaAl). Zeolite possesses small pore size and high acid sites, allowing for more selective cracking of smaller molecular compounds into light olefins and aromatics.

Deoxygenation of oxygenates mainly involves the decarboxylation of acetic acid and the dehydration of alcohol, where oxygen is removed via CO_2 and H_2O, respectively [38]. This was supported by the observed decline in the relative peak area of the acid from 11.43% to 7.65% to generate the maximum hydrocarbon content with an increase in the HAP-ZE-to-feedstock ratio from 1:10 to 1:6. The outstanding catalytic activity of HAP-ZE was due to the presence of base sites, such as calcium, which helped to promote deacidification of bio-oil via three reaction pathways, namely, neutralisation, thermal cracking, and catalytic cracking. The neutralisation reaction facilitated the conversion of acids to ketone, while thermal and catalytic decomposition were accountable for transforming acids into hydrocarbon [39]. Since no ketone was detected in the bio-oil, it can be implied that the neutralisation reaction was insignificant in this research. The lowest yield of 4.87% of acid was obtained at the highest HAP-ZE to SB/HDPE ratio of 1:2, which indicated that the deacidification reaction was strongly affected by catalyst dosage and became more active at a higher catalyst dosage. Catalytic cracking with base catalyst of polyolefins would proceed via

carbocationic mechanism. Carbocations and carbenium ions were created by removing hydride ions from Lewis acid sites or protonating the hydrocarbon on Brønsted acid sites. Other than carbocation production, cracking, isomerisation, oligomerisation, cyclisation, and aromatisation can also occur over the acid sites. As oppose to base catalysis, catalytic cracking over an acid catalyst would occur via the carbenium ion mechanism [40]. The low level of acid compounds could enhance the quality of bio-oil since this compound can cause corrosion and reduce the heating value of the liquid to be utilised as transportation fuel.

By contrast, the fraction of aromatics had fluctuated markedly when the HAP-ZE to SB/HDPE ratio was increased. Lower proportion of aromatic was obtained in this study compared to the co-pyrolysis of plastic and biomass by utilising microporous zeolites because larger pore catalysts, such as HAP-ZE do not favour aromatisation. Aromatics are produced from olefin cyclisation at the catalytic sites and the production was accelerated by strong Brønsted acidity. In addition, the selectivity of aromatic compound strongly depends on pore size and acidic site density, as these two factors play vital roles in cracking and isomerisation of hydrocarbons [41].

Based on the above findings, the maximum amount of hydrocarbon with sensible liquid yield was achieved at moderate HAP-ZE-to-SB/HDPE ratio of 1:6. The most significant cracking and deoxygenation reaction was believed to occur under this condition. Excessive catalyst dosage was good for deacidification reaction and alcohol production, but detrimental to hydrocarbon production. Considering the recovery of hydrocarbons from waste SB and HDPE, the 1:6 ratio was chosen as the optimum catalyst-to-feedstock ratio to investigate the impact of another factor.

3.3. Influence of mass ratio of SB to HDPE on pyrolytic products

The effect of SB to HDPE mass ratio on product yield and condensable compounds of bio-oil was examined at various mass ratios of SB to HDPE of 100:0, 20:80, 40:60, 60:40, and 0:100. The HAP-ZE to SB/HDPE ratio and the reaction temperature were set at 1:6 and 600 °C, respectively. Fig. 5 (a) and (b) reveals the influence of SB to HDPE mass ratio on product yield and condensable compounds. Liquid product yield was boosted from 42.50 wt% to the maximum yield of 71.19 wt%, when the mass ratio of SB to HDPE was decreased from 100:0 to 40:60 due to the synergistic effect between HDPE and SB intermediates. In contrast, reducing the mass ratio of SB to HDPE led to a decline in the char yield. HDPE acts as a hydrogen supplier that helps accelerate the removal of side chain functional groups, known as the methoxyl groups, which can lead to the reduction of char yield. Hosoya et al. [42] reported that the methoxyl group is a key structure for lignin char formation. Compared to the saturated derivatives, unsaturated derivatives with C═C side chains exhibit higher polymerization reactivities, resulting in increased char formation.

The influence of SB to HDPE mass ratio on the condensable compounds of bio-oil was observed. As illustrated in Fig. 5 (b), hydrocarbon and alcohol are the primary products in the bio-oil. The hydrocarbon content was increased with the decreasing SB:HDPE ratio. The maximum hydrocarbon of 66% was obtained at SB to HDPE ratio of 40:60. The addition of hydrogen-rich HDPE could act as hydrogen donors and enhance the overall H/C_{eff} value of the feedstock, by keeping the hydrocarbon pool functioning for hydrocarbon production. The hydrocarbon pool generated from biomass pyrolysis was hydrogen deficient due to the low H/C_{eff} ratio (0 to 0.3). Hydrocarbon production

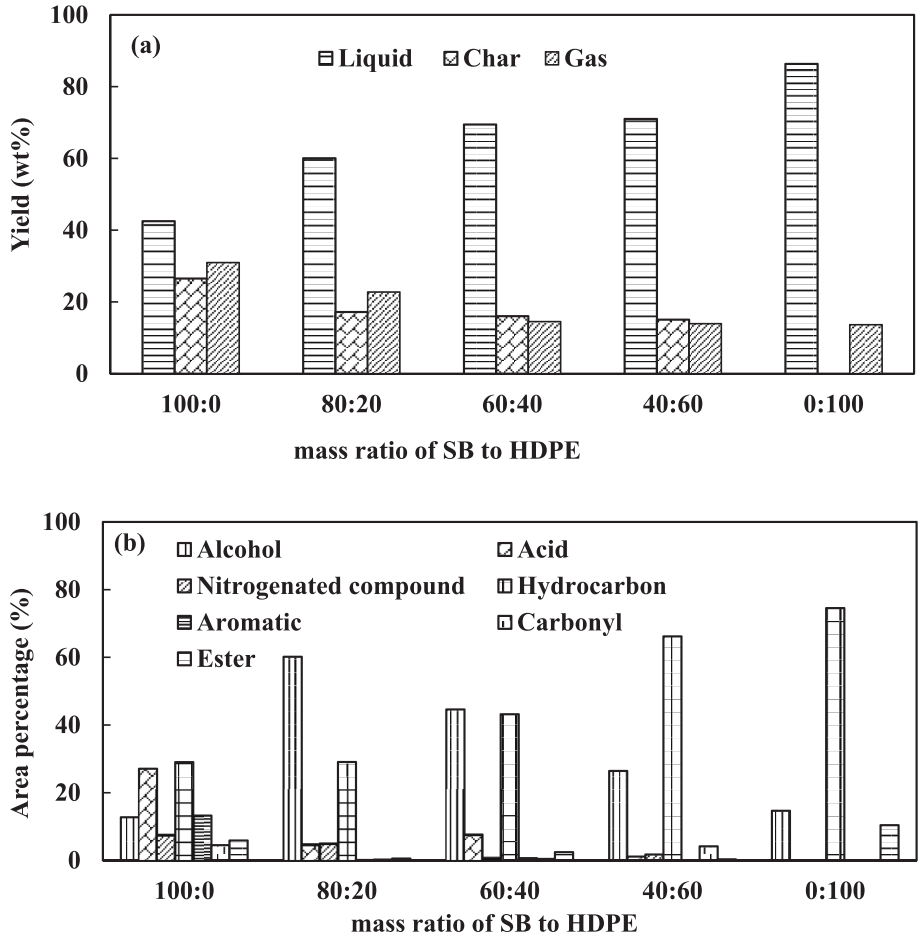

Fig. 5. Influence of mass ratio of SB to HDPE on (a) product yield and (b) condensable compounds of CCP of SB and HDPE over HAP-ZE.

can be intrinsically influenced by H/C_{eff} ratio, and feedstock that has a H/C_{eff} ratio of >1.0 could have a significant impact on hydrocarbon production [43].

The hydrocarbon content obtained in the present study was higher than the *co*-pyrolysis of torrefied rice straw and low density polyethylene (LDPE) over ZSM-5, with the maximum hydrocarbon yield of 40.22% [44]. The high amount of hydrocarbon found in the present study could be due to the differences in cracking and diffusion ability. The cracking and selectivity ability of the catalyst were strongly dependent on its acidity/basicity and porosity, as well as the structure of the polymer [40]. On the other hand, due to the nature of plastics, which possess high molecular weight molecules, their cracking and diffusion ability are influenced by the pore diameter and shape selectivity of the catalyst. HAP-ZE has a higher surface area and acidity compared to ZSM-5; therefore, it can provide more reaction space and acid sites for cracking and deoxygenation reactions. In addition, mesoporous HAP-ZE could allow more molecules to enter its active sites to undergo deoxygenation via hydrocarbon pool to produce more hydrocarbons. On the other hand, the structure of LDPE, which has more branches, tends to produce more wax than HDPE, which could affect the amount of hydrocarbon produced. The hydrocarbon derived from catalytic co-pyrolysis over HAP-ZE can be classified into alkanes (aliphatic), alkene (olefin), and alkynes. The most dominant hydrocarbon compound in the bio-oil was aliphatic (43.53%), which included Eicosane, Heneicosane, and Nonadecane. These alkanes were produced via the decarboxylation of acid, and the decarbonylation of sugar and hydrogenation of HDPE-derived alkene.

The oxygenates had dramatically decreased with the addition of 60% of HDPE, specifically acid (from 27.07% to 1.12%), and ester (from 5.87% to 0%). The increase in HDPE portion encouraged the transformation of oxygenates to hydrocarbon, with decarboxylation being one among the pathways involved. On the other hand, alcohol yield was reduced at the expense of hydrocarbon, suggesting that an increment of HDPE portion in the feedstock had inhibited the production of alcohol. The alcohol yield was decreased from 60.1% to 26.42% when the SB:HDPE ratio was decreased from 80:20 to 40:60. The increased HDPE portion in the feedstock had supplied more hydrogen radicals and amplified the H/C_{eff} ratio of the feedstock, which effectively enhanced the conversion of alcohol into hydrocarbon via the dehydration reaction. When the amount of aromatic compound was decreased and gradually diminished when the SB:HDPE ratio was decreased, the addition of HDPE could have had a lesser impact on aromatic quantity. This phenomenon was due to the enhancement of C—C coupling reaction that transformed carboxylic acid into alkanes and not olefins, which reduced the aromatic proportion in bio-oil [45]. The HDPE acted as a superior co-reactant to SB in balancing the yield and quality of bio-oil via hydrogen donor. A greater HDPE fraction (60%) proved good for accelerating hydrocarbon synthesis and decreasing oxygenates, hence improving bio-oil quality. Thus, the optimal plastic ratio in the catalytic co-pyrolysis over HAP-ZE was 60%.

The plausible chemical pathway during the catalytic co-pyrolysis over HAP-ZE was shown in Scheme 1. The SB breakdown took place at lower temperatures than degradation of HDPE through a series of exothermic and endothermic reactions. These reactions would produce various oxygenated compounds (acid, sugar, and alcohol and ester), and reactive free radicals, for example, hydroxyl radicals ($^{-}$OH). Acid was formed via the ring opening of cellulose- and hemicellulose-derived anhydro saccharides, while sugar (mainly levoglucosan) was produced by the breakdown of a glycosidic bond of cellulose. When the temperature was elevated, the pyrolysis of HDPE occurred via carbonium ions and β-scission reaction to generate long chains of hydrocarbon together with alcohol and ester. The SB-derived oxygenates and hydroxyl radicals ($^{-}$OH) also helped initiate the decomposition of HDPE via hydrogen abstraction to generate aliphatic hydrocarbon with activated H^{+} of different chain lengths. The HDPE-derived H^{+} could interact with hydroxyl radicals ($^{-}$OH) to form linear, long-chain alcohols, namely, 1-Decanol, 2-hexyl-, 1-Eicosanol, and 1-Heptacosanol.

Acid sites of HAP-ZE facilitated the hydrogenation of HDPE-derived olefins to alkane (Eicosane, Heneicosane, Nonadecane) and deoxygenation of SB and HDPE derived intermediates via the hydrocarbon pool

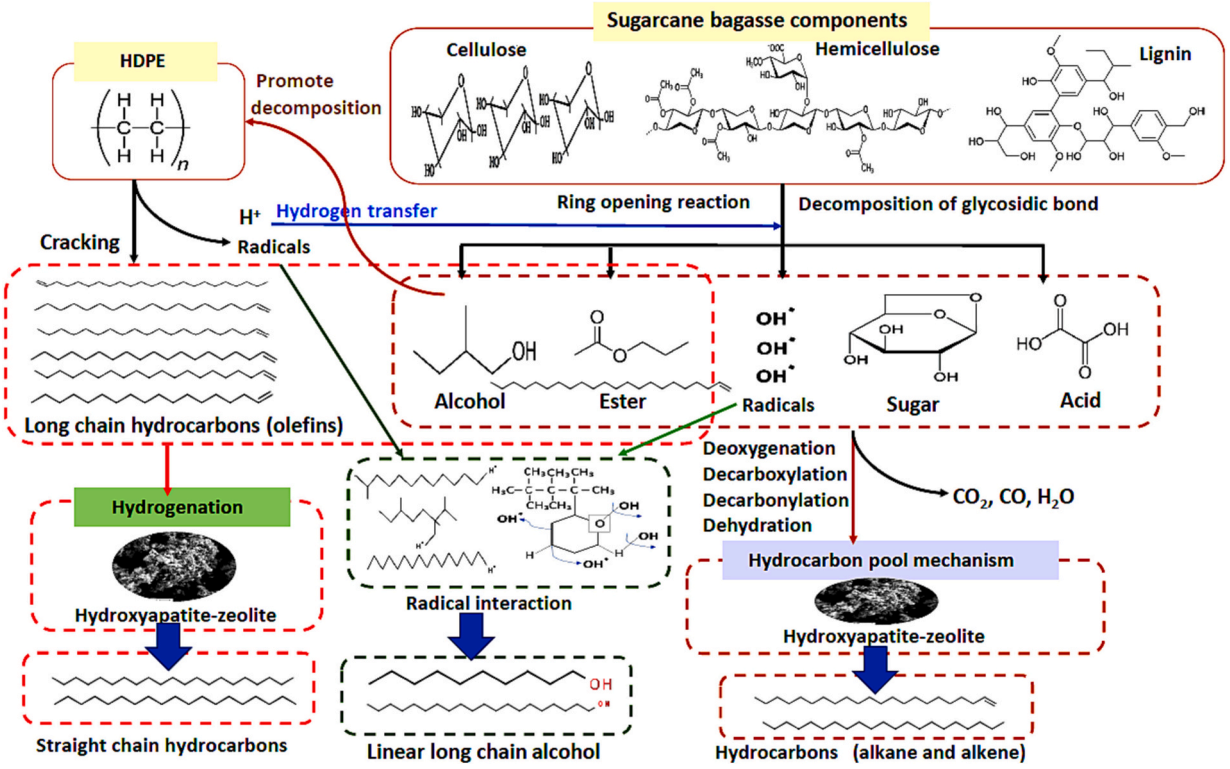

Scheme 1. Plausible reaction pathway for the synthesis of key chemicals via catalytic co-pyrolysis of SB and HDPE.

mechanism. In this mechanism, the oxygenated compounds were diffused into the HAP-ZE pores to undergo deoxygenation process via dehydration, decarbonylation, and decarboxylation into hydrocarbons, such as alkane and alkene. In addition, the olefins derived from HDPE decomposition that acted as hydrogen supplements had also obtained admission into the hydrocarbon pool, which kept it active and reactive to non-furanic products to produce more hydrocarbons. This condition had resulted in the reduced generation of oxygen-containing compounds in the liquid product and enhanced the production of hydrocarbons. Furthermore, the basic sites of HAP-ZE had also enhanced the deoxygenation reactions including decarboxylation and decarbonylation through electron shift, which further reduced the portion of acid in bio-oil.

4. Conclusion

Mesoporous HAP-ZE derived from steel waste was found to be effective in the cracking and deoxygenation of SB and HDPE pyrolyzates, favouring the formation of hydrocarbon and the reduction of acid. The maximum liquid yield of 71.19 wt% was obtained at HAP-ZE to SB/HDPE ratio of 1:6, and SB to HDPE ratio of 40:60. The meso-porosity and high surface area of the HAP-ZE had enhanced the passage of bulky intermediates molecules into the channels of the catalyst, and eased the cracking and deoxygenation of intermediate pyrolyzates, thus, forming more hydrocarbons. The formation of hydrocarbon can be ascribed to the hydrocarbon pool mechanism, since the main SB-derived oxygenated compounds are non-furanic components, including anhydrosugar and acetic acid. HDPE could act as hydrogen donors and enhance the overall H/C_{eff} value of the feedstock, by keeping the hydrocarbon pool functioning for hydrocarbon production. The acid sites promoted the hydrogenation and deoxygenation via hydrocarbon pool while the basic sites promoted the deoxygenation reactions via decarboxylation and decarbonylation reactions. The presence of basic sites of HAP-ZE helped reduced the acid portion of the CCP bio-oil. The resultant liquid product was rich in hydrocarbon (66.19%) and alcohol (26.42%), with minimum amounts of acid (1.12%) and nitrogenated compounds (1.74%). The presence of both hydrocarbon and alcohol in the bio-oil was appealing for the prospect of utilising it as transportation fuel. The hydrocarbon in the bio-oil increases its stability and heating value, while the alcohol enhances the octane number.

CRediT authorship contribution statement

H. Hassan: Investigation, Formal analysis, Data curation, Writing - original draft, Writing - review & editing. **B.H. Hameed:** Validation, Funding acquisition, Writing - review & editing, Supervision.

Declaration of Competing Interest

The authors affirm that there are no known competing financial interests or personal relationships that could have influenced the reported work in this paper.

Data availability

Data will be made available on request.

Acknowledgements

The first author expresses gratitude for the scholarship support received from the Ministry of Higher Education (MOHE), Malaysia . The authors thankfully acknowledge the support obtained from Universiti Sains Malaysia in the form of research facilities.

Appendix A. Supplementary data

Supplementary data to this article can be found online at https://doi.org/10.1016/j.catcom.2023.106795.

References

[1] J. Jin, J. Sun, K. Lv, Q. Hou, X. Guo, K. Liu, Y. Deng, L. Song, Catalytic pyrolysis of oil shale using tailored cu@zeolite catalyst and molecular dynamic simulation, Energy. 278 (2023), https://doi.org/10.1016/j.energy.2023.127858.
[2] H. Yang, J. Zhang, Z. Chen, L. Wan, C. Li, X. Zhang, J. Li, R. Tian, J. Yu, S. Gao, Base-acid relay catalytic upgrading of coal pyrolysis volatiles over CaO and HZSM-5 catalysts, J. Anal. Appl. Pyrolysis 170 (2023), 105926, https://doi.org/10.1016/j.jaap.2023.105926.
[3] Y.L. Tan, B.H. Hameed, A.Z. Abdullah, Deoxygenation of pyrolysis vapour derived from durian shell using catalysts prepared from industrial wastes rich in Ca, Fe, Si and Al Y.L, Sci. Total Environ. 702 (2020), 134902, https://doi.org/10.1016/0048-9697(87)90257-9.
[4] Y. Zheng, J. Wang, C. Liu, X. Lin, Y. Lu, W. Li, Z. Zheng, Enhancing the aromatic hydrocarbon yield from the catalytic copyrolysis of xylan and LDPE with a dual-catalytic-stage combined CaO/HZSM-5 catalyst, J. Energy Inst. 93 (2020) 1833–1847, https://doi.org/10.1016/j.joei.2020.03.014.
[5] D.T. Sekyere, J. Zhang, Y. Chen, Y. Huang, M. Wang, J. Wang, N. Niwamanya, A. Barigye, Y. Tian, Production of light olefins and aromatics via catalytic co-pyrolysis of biomass and plastic, Fuel. 333 (2023), 126339, https://doi.org/10.1016/j.fuel.2022.126339.
[6] J. Zhang, Y.S. Choi, B.H. Shanks, Catalytic deoxygenation during cellulose fast pyrolysis using acid-base bifunctional catalysis, Catal. Sci. Technol. 6 (2016) 7468–7476, https://doi.org/10.1039/c6cy01307d.
[7] S. Shao, P. Zhang, X. Xiang, X. Li, H. Zhang, Promoted ketonization of bagasse pyrolysis gas over red mud-based oxides, Renew. Energy 190 (2022) 11–18, https://doi.org/10.1016/j.renene.2022.02.105.
[8] H.S. Heo, S. Pyo, B.S. Kang, J.S. Jung, G.H. Rhee, Y.M. Kim, J.M. Kim, Y.K. Park, Synthesis of biofuel via catalytic fast pyrolysis of wood-plastic composite over low-cost catalysts, Sustain. Energ. Technol. Assess. 56 (2023) 1–6, https://doi.org/10.1016/j.seta.2023.103051.
[9] Z. Wan, Z. Li, W. Yi, A. Zhang, G. Li, S. Wang, Lignin and spent bleaching clay into mono-aromatic hydrocarbons by a cascade dual catalytic pyrolysis system: critical role of spent bleaching clay, Int. J. Biol. Macromol. 236 (2023), 123879, https://doi.org/10.1016/j.ijbiomac.2023.123879.
[10] A.M. Novack, T.C. Costa, F.V. Hackbarth, B.A. Marinho, A.U. Souza, V.J.P. Vilar, S. M.A. Guelli, U. Souza, B. Valle, Industrial steel waste recovery pathway : production of innovative supported catalyst and its application on hexavalent chromium reduction studies, Chemosphere. 298 (2022), 134216.
[11] S. Hosseini, S.M. Soltani, P.S. Fennell, T.S.Y. Choong, M.K. Aroua, Production and applications of electric-arc-furnace slag as solid waste in environmental technologies: a review, Environ. Technol. Rev. 5 (2016) 1–11, https://doi.org/10.1080/21622515.2016.1147615.
[12] B. Rego, D. Vasconcelos, D. Pham, E. Martins, A. Germeau, P. Sharrock, A. Nzihou, Highly-efficient hydroxyapatite-supported nickel catalysts for dry reforming of methane, Int. J. Hydrog. Energy 45 (2019) 18502–18518, https://doi.org/10.1016/j.ijhydene.2019.08.068.
[13] C. Chen, D. Fan, J. Zhao, Q. Qi, X. Huang, T. Zeng, Y. Bi, Study on microwave-assisted co-pyrolysis and bio-oil of Chlorella vulgaris with high-density polyethylene under activated carbon, Energy. 247 (2022), 123508.
[14] M.R. Errera, T.A.D.C. Dias, D.M.Y. Maya, E.E.S. Lora, Global bioenergy potentials projections for 2050, Biomass Bioenergy 170 (2023), https://doi.org/10.1016/j.biombioe.2023.106721.
[15] C. Chen, D. Fan, H. Ling, X. Huang, G. Yang, D. Cai, J. Zhao, Y. Bi, Microwave catalytic co-pyrolysis of Chlorella vulgaris and high density polyethylene over activated carbon supported monometallic: characteristics and bio-oil analysis, Bioresour. Technol. 363 (2022), 127881.
[16] H. Ahmed, M.T.H. Siddiqui, S. Nizamuddin, N.M. Mubarak, M. Khalid, M. P. Srinivasan, G.J. Griffin, Solvothermal co-liquefaction of sugarcane bagasse and polyethylene under sub-supercritical conditions : optimization of process parameters, Process. Saf. Environ. Prot. 137 (2020) 300–311.
[17] N. Azlina, M. Jawaid, E. Syams, S. Abdul, K. Yamani, Tensile , physical and morphological properties of oil palm empty fruit bunch/ sugarcane bagasse fibre reinforced phenolic hybrid composites, J. Mater. Res. Technol. 8 (2019) 3466–3474.
[18] P. Ghorbannezhad, S. Park, J.A. Onwudili, Co-pyrolysis of biomass and plastic waste over zeolite- and sodium-based catalysts for enhanced yields of hydrocarbon products, Waste Manag. 102 (2020) 909–918, https://doi.org/10.1016/j.wasman.2019.12.006.
[19] J. Xu, N. Brodu, L. Abdelouahed, B. Taouk, Investigation of the combination of fractional condensation and water extraction for improving the storage stability of pyrolysis bio-oil, Fuel. 314 (2022) 1–37, https://doi.org/10.1016/j.fuel.2021.123019.
[20] H. Ghai, D. Sakhuja, S. Yadav, P. Solanki, C. Putatunda, R.K. Bhatia, A.K. Bhatt, S. Varjani, Y.H. Yang, S.K. Bhatia, A. Walia, An overview on co-pyrolysis of biodegradable and non-biodegradable wastes, Energies. 15 (2022) 1–27, https://doi.org/10.3390/en15114168.
[21] M.H.M. Ahmed, N. Batalha, H.M.D. Mahmudul, G. Perkins, M. Konarova, A review on advanced catalytic co-pyrolysis of biomass and hydrogen-rich feedstock:

insights into synergistic effect, catalyst development and reaction mechanism, Bioresour. Technol. 310 (2020), 123457, https://doi.org/10.1016/j.biortech.2020.123457.
[22] W.A. Khanday, F. Marrakchi, M. Asif, B.H. Hameed, Mesoporous zeolite – activated carbon composite from oil palm ash as an effective adsorbent for methylene blue, J. Taiwan Inst. Chem. Eng. 70 (2017) 32–41.
[23] N. Iqbal, M.R. Abdul Kadir, N.H. Bin Mahmood, M.F.M. Yusoff, J.A. Siddique, N. Salim, G.R.A. Froemming, M.N. Sarian, H.R. Balaji Raghavendran, T. Kamarul, Microwave synthesis, characterization, bioactivity and in vitro biocompatibility of zeolite-hydroxyapatite (Zeo-HA) composite for bone tissue engineering applications, Ceram. Int. 40 (2014) 16091–16097, https://doi.org/10.1016/j.ceramint.2014.07.038.
[24] Y. Kuwahara, T. Ohmichi, T. Kamegawa, K. Mori, H. Yamashita, A novel synthetic route to hydroxyapatite-zeolite composite material from steel slag: investigation of synthesis mechanism and evaluation of physicochemical properties, J. Mater. Chem. 19 (2009) 7263–7272, https://doi.org/10.1039/b911177h.
[25] G. Kabir, A.T. Mohd Din, B.H. Hameed, Pyrolysis of oil palm mesocarp fiber catalyzed with steel slag-derived zeolite for bio-oil production, Bioresour. Technol. 249 (2018) 42–48, https://doi.org/10.1016/j.neubiorev.2017.04.006.
[26] T. Jose, J. Ftouni, P.C.A. Bruijnincx, Structured hydroxyapatite composites as efficient solid base catalysts for condensation reactions, Catal, Sci. Technol. 11 (2021) 3428–3436, https://doi.org/10.1039/D1CY00102G.
[27] G.U. Ryu, G.M. Kim, H.R. Khalid, H.K. Lee, The effects of temperature on the hydrothermal synthesis of hydroxyapatite-zeolite using blast furnace slag, Materials (Basel, Switzerland) vol. 12 (2019) 2131, https://doi.org/10.3390/ma12132131.
[28] K. Na, G.A. Somorjai, Hierarchically Nanoporous zeolites and their heterogeneous catalysis: current status and future perspectives, Catal. Lett. 145 (2015) 193–213, https://doi.org/10.1007/s10562-014-1411-5.
[29] B. Kaur, R. Srivastava, B. Satpati, K.K. Kondepudi, M. Bishnoi, Biomineralization of hydroxyapatite in silver ion-exchanged nanocrystalline ZSM-5 zeolite using simulated body fluid, Colloids Surf. B: Biointerfaces 135 (2015) 201–208, https://doi.org/10.1016/j.colsurfb.2015.07.068.
[30] K.A. Cychosz, M. Thommes, Progress in the Physisorption characterization of Nanoporous gas storage materials, Engineering. 4 (2018) 559–566, https://doi.org/10.1016/j.eng.2018.06.001.
[31] W. Yao, J. Li, Y. Feng, W. Wang, X. Zhang, Q. Chen, S. Komarneni, Y. Wang, Thermally stable phosphorus and nickel modified ZSM-5 zeolites for catalytic co-pyrolysis of biomass and plastics, RSC Adv. 5 (2015) 30485–30494, https://doi.org/10.1039/c5ra02947c.
[32] H. Hassan, B.H. Hameed, J.K. Lim, Co-pyrolysis of sugarcane bagasse and waste high-density polyethylene: synergistic effect and product distributions, Energy. 191 (2020), 116545, https://doi.org/10.1016/j.energy.2019.116545.
[33] Y. Zhao, Y. Wang, D. Duan, R. Ruan, L. Fan, Y. Zhou, L. Dai, J. Lv, Y. Liu, Fast microwave-assisted ex-catalytic co-pyrolysis of bamboo and polypropylene for bio-oil production, Bioresour. Technol. 249 (2018) 69–75.
[34] Y. Wang, L. Dai, L. Fan, L. Cao, Y. Zhou, Y. Zhao, Y. Liu, R. Ruan, Catalytic co-pyrolysis of waste vegetable oil and high density polyethylene for hydrocarbon fuel production, Waste Manag. 61 (2017) 276–282, https://doi.org/10.1016/j.wasman.2017.01.010.
[35] M.V. Rocha, A.J. Vinuesa, L.B. Pierella, M.S. Renzini, Enhancement of bio-oil obtained from co-pyrolysis of lignocellulose biomass and LDPE by using a natural zeolite, Therm. Sci. Eng. Progress. 19 (2020), 100654, https://doi.org/10.1016/j.tsep.2020.100654.
[36] G.T.M. Kadja, M.M. Ilmi, N.J. Azhari, M. Khalil, A.T.N. Fajar, I.G.B.N. Subagjo, M. L. Makertihartha, C.B. Gunawan, I.G. Wenten Rasrendra, Recent advances on the nanoporous catalysts for the generation of renewable fuels, J. Mater. Res. Technol. 17 (2022) 3277–3336, https://doi.org/10.1016/j.jmrt.2022.02.033.
[37] H.W. Ryu, Y.F. Tsang, H.W. Lee, J. Jae, S.C. Jung, S.S. Lam, E.D. Park, Y.K. Park, Catalytic co-pyrolysis of cellulose and linear low-density polyethylene over MgO-impregnated catalysts with different acid-base properties, Chem. Eng. J. 373 (2019) 375–381, https://doi.org/10.1016/j.cej.2019.05.049.
[38] T. Sun, T. Lei, Z. Li, Z. Zhang, S. Yang, X. Xin, M. Zhang, X. He, Q. Zhang, L. Zhang, Catalytic co-pyrolysis of corn stalk and polypropylene over Zn-Al modified MCM-41 catalysts for aromatic hydrocarbon-rich oil production, Ind. Crop. Prod. 171 (2021), 113843, https://doi.org/10.1016/j.indcrop.2019.111613.
[39] L.M. Orozco, M. Renz, A. Corma, Cerium oxide as a catalyst for the ketonization of aldehydes: mechanistic insights and a convenient way to alkanes without the consumption of external hydrogen, Green Chem. 19 (2017) 1555–1569, https://doi.org/10.1039/C6GC03511F.
[40] K. Saeaung, N. Phusunti, W. Phetwarotai, S. Assabumrungrat, B. Cheirsilp, Catalytic pyrolysis of petroleum-based and biodegradable plastic waste to obtain high-value chemicals, Waste Manag. 127 (2021) 101–111, https://doi.org/10.1016/j.wasman.2021.04.024.
[41] N. Miskolczi, F. Ateş, Thermo-catalytic co-pyrolysis of recovered heavy oil and municipal plastic wastes, J. Anal. Appl. Pyrolysis 117 (2016) 273–281, https://doi.org/10.1016/j.jaap.2015.11.005.
[42] T. Hosoya, H. Kawamoto, S. Saka, Role of methoxyl group in char formation from lignin-related compounds, J. Anal. Appl. Pyrolysis 84 (2009) 79–83, https://doi.org/10.1016/j.jaap.2008.10.024.
[43] Z.B. Zhang, Q. Lu, X.N. Ye, W.T. Li, B. Hu, C.Q. Dong, Production of phenolic-rich bio-oil from catalytic fast pyrolysis of biomass using magnetic solid base catalyst, Energy Convers. Manag. 106 (2015) 1309–1317, https://doi.org/10.1016/j.enconman.2015.10.063.
[44] Q. Bu, Y. Liu, J. Liang, H.M. Morgan, L. Yan, F. Xu, H. Mao, Microwave-assisted co-pyrolysis of microwave torrefied biomass with waste plastics using ZSM-5 as a catalyst for high quality bio-oil, J. Anal. Appl. Pyrolysis 134 (2018) 536–543, https://doi.org/10.1016/j.jaap.2018.07.021.
[45] E.I. Gürbüz, E.L. Kunkes, J.A. Dumesic, Integration of C-C coupling reactions of biomass-derived oxygenates to fuel-grade compounds, Appl. Catal. B Environ. 94 (2010) 134–141, https://doi.org/10.1016/j.apcatb.2009.11.001.